Assessment of First- and Second-Order Wave-Excitation Load Models for Cylindrical Substructures

Preprint

Brandon Pereyra, Fabian Wendt,
Amy Robertson, and Jason Jonkman
National Renewable Energy Laboratory

Presented at the International Society of Offshore and Polar Engineers Conference (ISOPE 2016)
Rhodes, Greece
June 26–July 2, 2016

NREL is a national laboratory of the U.S. Department of Energy
Office of Energy Efficiency & Renewable Energy
Operated by the Alliance for Sustainable Energy, LLC

This report is available at no cost from the National Renewable Energy Laboratory (NREL) at www.nrel.gov/publications.

Conference Paper
NREL/CP-5000-68131
March 2017

Contract No. DE-AC36-08GO28308

NOTICE

This report is available at no cost from the National Renewable Energy Laboratory (NREL) at www.nrel.gov/publications.

Available electronically at SciTech Connect http:/www.osti.gov/scitech

Available for a processing fee to U.S. Department of Energy and its contractors, in paper, from:

U.S. Department of Energy
Office of Scientific and Technical Information
P.O. Box 62
Oak Ridge, TN 37831-0062
OSTI http://www.osti.gov
Phone: 865.576.8401
Fax: 865.576.5728
Email: reports@osti.gov

Available for sale to the public, in paper, from:

U.S. Department of Commerce
National Technical Information Service
5301 Shawnee Road
Alexandria, VA 22312
NTIS http://www.ntis.gov
Phone: 800.553.6847 or 703.605.6000
Fax: 703.605.6900
Email: orders@ntis.gov

Cover Photos by Dennis Schroeder: (left to right) NREL 26173, NREL 18302, NREL 19758, NREL 29642, NREL 19795.

NREL prints on paper that contains recycled content.

Note: This is a revision of the original paper presented at ISOPE 2016.

ISOPE-2016 Proceedings — Assessment of First- and Second-Order Wave-Excitation Load Models for Cylindrical Substructures

Brandon Pereyra, Fabian Wendt, Amy Robertson, Jason Jonkman
National Renewable Energy Laboratory
Golden, Colorado, USA

ABSTRACT

The hydrodynamic loads on an offshore wind turbine's support structure present unique engineering challenges for offshore wind. Two typical approaches used for modeling these hydrodynamic loads are potential flow (PF) and strip theory (ST), the latter via Morison's equation. This study examines the first- and second-order wave-excitation surge forces on a fixed cylinder in regular waves computed by the PF and ST approaches to (1) verify their numerical implementations in HydroDyn and (2) understand when the ST approach breaks down. The numerical implementation of PF and ST in HydroDyn, a hydrodynamic time-domain solver implemented as a module in the FAST wind turbine engineering tool, was verified by showing the consistency in the first- and second-order force output between the two methods across a range of wave frequencies. ST is known to be invalid at high frequencies, and this study investigates where the ST solution diverges from the PF solution. Regular waves across a range of frequencies were run in HydroDyn for a monopile substructure. As expected, the solutions for the first-order (linear) wave-excitation loads resulting from these regular waves are similar for PF and ST when the diameter of the cylinder is small compared to the length of the waves (generally when the diameter-to-wavelength ratio is less than 0.2). The same finding applies to the solutions for second-order wave-excitation loads, but for much smaller diameter-to-wavelength ratios (based on wavelengths of first-order waves).

KEY WORDS: Hydrodynamics; monopile; second-order forces; potential flow; strip theory

INTRODUCTION

Offshore wind turbines are more complex than land-based turbines due to hydrodynamic loads and the corresponding structural responses (Musial and Ram, 2010). There are different methods for calculating the wave loads on structures. The HydroDyn hydrodynamics module in FAST—an open-source engineering tool developed by the National Renewable Energy Laboratory (Jonkman, Roberston, and Hayman, 2014) to support offshore wind energy technology development—allows for two different hydrodynamic modeling techniques to be used: potential flow (PF) and strip theory (ST). For PF, frequency-dependent hydrodynamic coefficients are required as inputs to HydroDyn, commonly calculated from the Wave Analysis at the Massachusetts Institute of Technology (WAMIT) software (Lee, 1995). For ST, hydrodynamic loads are calculated in HydroDyn using a generalized form of Morison's equation based on undisturbed wave kinematics and constant user-specified hydrodynamic coefficients.

The PF solution is applicable to situations where the flow does not separate and for substructures or members of substructures that are large relative to a typical wavelength. The ST solution is preferable in situations where flow separation occurs and for substructures or members of substructures that are small in diameter relative to a typical wavelength.

The focus of our study is to understand the differences in the wave-excitation loads calculated by these two hydrodynamic theories (PF and ST) for both first- and second-order waves. Within FAST (HydroDyn), the hydrodynamic theories account for several load components, including hydrostatic, radiation (both added mass and damping in PF, only added mass in ST), viscous drag (only in ST, not PF), Froude-Kriloff, and scattering loads (diffraction in PF, long-wavelength approximation in ST). Further, second-order contributions to each load component increase the complexity and accuracy of the solution, especially in severe sea states. The magnitude and frequency content of second-order hydrodynamic loads can excite structural natural frequencies, leading to greater ultimate and fatigue loads than can be predicted solely using first-order theory. Sum-frequency effects are important to the loading of stiff fixed-bottom structures and for the springing and ringing analysis of tension-leg platforms (TLPs). Difference-frequency (mean-drift and slow-drift) effects are important to the analysis of compliant structures, including the motion analysis and mooring loads of catenary-moored floating platforms (spar buoys and semi-submersibles).

In this study, we focus only on the first- and second-order wave-excitation (also referred to as *inertia* or *diffraction*) force components under regular waves, which include the combined contribution of the first- and second-order Froude-Kriloff and scattering terms. For regular waves, first-order components oscillate at the wave frequency, second-order sum-frequency forces oscillate at twice the wave frequency, and the second-order difference-frequency force is a constant mean-drift force. In general, second-order terms include contributions from both the second-order potential and the quadratic interaction of first-order terms, but only the quadratic term affects the mean-drift force (Faltinsen, 1990).

To compare the differences between the PF and ST models, a series of simulations were run at different regular wave frequencies with the monopile offshore wind substructure used in the Offshore Code Comparison Collaboration (OC3) project (Jonkman and Musial, 2010). Both the first- and second-order wave-excitation surge forces were calculated. Differences between ST and PF for the first-order solution are documented and readily understood. Because of the long wavelength approximation used by Morison's equation in ST, first-order solutions for PF and ST are expected to match at low frequencies and diverge at high frequencies—when the ratio of the diameter of the cylinder over the wavelength increases above 0.2. Differences between ST and PF for the second-order solution are less well known and are the central aspect of this analysis.

To focus on the basic differences between the theories, a number of simplifying assumptions were made. No wave stretching was considered (wave forces were calculated only up to the still-water level (SWL)). Waves were modeled using regular (not irregular/stochastic) wave theory, and only the force (not moment) in the wave direction was analyzed. In addition, the second-order wave kinematics (Stokes theory) used in the ST solution included only the solution of the second-order potential, not the quadratic interaction of first-order terms (which were included in the PF solution).

MATERIALS AND METHODS

Cylindrical Model and Discretization

The hydrodynamic wave-excitation forces on the fixed OC3-monopile cylindrical model were investigated and modeled in HydroDyn. The geometric properties and numerical discretization of this model are listed in Table 1. The cylinder extended from the SWL to the seabed, so the cylinder length was equal to the water depth; without considering wave stretching, there was no need to extend the model above the water.

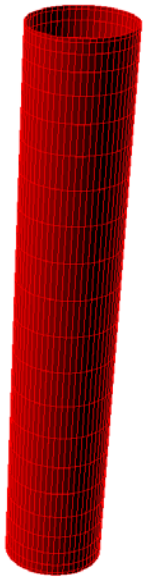

Fig 1. Panel mesh of the OC3 monopile

For the PF solution in WAMIT, a mesh of the cylinder was required; and for the second-order PF solution, a mesh of the water's free surface was required in addition to the cylindrical mesh. Only the curved cylindrical surfaces had to be meshed because the bottom surface was not exposed to the water. Because of geometrical symmetry, only one-quarter of the cylinder was meshed. Higher-order geometry files were used in this study because they required fewer panels to achieve convergence of surge forces compared to low-order flat panels. Third-order splines were used to model the higher-order panels. In addition to higher-order panels, nonuniform spacing was used to increase resolution at the edges of the cylinder (Fig 1). For the automated free-surface mesh generation, the ratio of the length of the water line panels to the free-surface mesh panels was set to unity. The free-surface mesh was extended in the radial directions three times the size of the cylinder's diameter.

For the ST model in HydroDyn, the geometry was discretized into cylindrical members and joints. These members were evenly spaced with lengths of 0.1 m.

Table 1. Cylindrical structure properties being modeled

Properties	OC3 Monopile
Diameter (m)	6
Water Depth (m)	20
Number of PF panels (covering ¼ of body)	200
Number of ST nodes	201

Potential-Flow Solution

For the PF simulations in HydroDyn, the following terms were extracted from the WAMIT model: the wave-excitation force response amplitude operators from the first-order problem and the second-order difference- and sum-frequency wave-excitation force quadratic transfer functions from the combined effects of the second-order potential and quadratic interaction of first-order terms. HydroDyn was then used to compute the time-varying hydrodynamic loads and system responses for a given sea state from these frequency-dependent force coefficients.

A convergence study was performed in WAMIT to determine the mesh's influence on the PF solution. Differently sized meshes were used for the simulation, and the percent deviations among the solutions were analyzed. Our convergence study used 8, 49, and 200 higher-order panels covering one-quarter of the cylinder surface. Convergence with the 200-panel meshes was confirmed visually by comparing surge forces among a broad range of frequencies for both first- and second-order forces.

Strip-Theory Solution

For the ST solution in HydroDyn, only the wave-excitation force term was calculated to focus our comparison. This was done by setting the drag coefficient to zero and by disabling all structural degrees of freedom. The inertia coefficient was set to two (one plus an added-mass coefficient of one). Although an added-mass coefficient of one is known to be valid only at low frequencies, we wanted to use our study to identify where ST and PF diverge as a result of that setting. Future work could look at whether using a smaller (and frequency-dependent) added-mass coefficient could better match ST to PF at high frequencies.

Analysis

Because waves cause an oscillating surge force on fixed structures, the main physical property investigated was the amplitude of these force oscillations. Both the PF and ST methods were used to calculate the first- and second-order components of the wave force amplitudes. The solutions extracted from the simulations for comparison were the amplitudes of the force responses for regular wave frequencies ranging from 0.016 Hz to 0.5 Hz.

The force amplitudes for both PF and ST were calculated using three methods to ensure that each method was consistent. For PF, the three methods to calculate the force amplitudes included:

- analyzing the power spectral density (PSD) of the force signal (described next),
- separating out the first- and second-order force components and finding the maximum and minimum force of the periodic steady-state signals, and
- calculating the force directly from the WAMIT output hydrodynamic coefficients.

The PSD of the force signal was calculated as the square of the Fourier transform; the first- and second-order force components were then found by integrating the first and second peak in the PSD. All of the PF

methods used to calculate the force amplitudes yielded equivalent PF results across all frequencies. The three methods used for the ST solution were:

- PSD peak integration,
- minimum and maximum force values, and
- the first- and second-order theoretical ST solutions for fixed structures, which were derived from Eqs. 5–7 shown in the appendix.

All of the ST methods yielded equivalent results across all frequencies.. This step verified the numerical implementation of the various methods within HydroDyn. With all of the methods giving equivalent results, the method used to calculate the force amplitude shown in the results below was to take the maximum and minimum force from the periodic steady-state force components output from HydroDyn.

RESULTS AND DISCUSSION

Normalized Force Amplitudes

The calculated first- and second-order wave-excitation normalized force amplitudes are displayed in Fig. 2 for the OC3 monopile as a function of the first-order wave frequency and cylinder diameter-to-wavelength ratio. The first-order force amplitudes (1st), represented by dashed lines, were normalized by the first-order wave amplitude. The second-order force amplitudes (2nd) were normalized by the first-order wave amplitude squared. For the second-order force amplitudes from PF, Fig. 3 shows the separate contributions to the total (Total). These components are the sum-frequency force from the quadratic interaction of first-order terms (Quadratic); the sum-frequency force from the second-order potential (Potential); and the difference-frequency component (Mean drift), the latter of which consists of only the quadratic contribution because the potential contribution to the difference-frequency component in regular waves is zero. Fig. 3 shows that the second-order quadratic and potential contributions can be larger than the total second-order force because the individual contributions can be out of phase with each other.

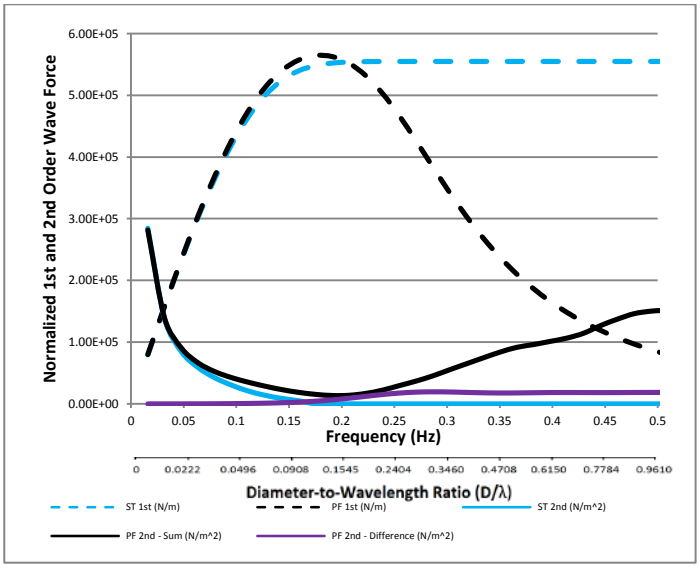

Fig 2. PF- and ST-generated normalized first- and second-order hydrodynamic force amplitudes on the OC3 monopile

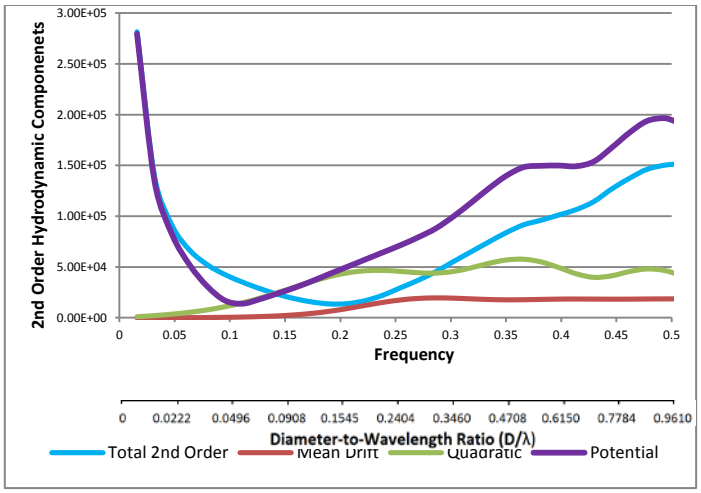

Fig 3. Quadratic and potential components of the normalized second-order hydrodynamic sum terms shown on the OC3 monopile. The second-order hydrodynamic difference term (mean drift) is also displayed.

Across the frequency range from 0.016 Hz to 0.222 Hz and the corresponding cylinder diameter-to-wavelength ratio range from 0.007 to 0.191, the PF- and ST-generated first-order force amplitudes are similar, with differences less than 5% (Fig. 2). For frequencies larger than 0.222 Hz, the first-order amplitudes deviate much more. As expected, this demonstrates that PF and ST match at low frequencies and diverge because of the long wavelength approximation in ST when the cylinder diameter-to-wavelength ratio increases above 0.2.

The second-order solutions diverge around 0.05 Hz, corresponding to a 0.022 diameter-to-wavelength ratio. These results show that the second-order solution diverges at a frequency of approximately one-quarter of the wave frequency that the first-order solution diverges. The second-order sum-frequency forces oscillate at twice the frequency of the first-order force. This means that the "effective" wavelength of the second-order sum-frequency terms are approximately one-quarter of the first-order wavelength, leading us to believe that second-order sum-frequency divergence follows the same diameter-to-wavelength rule of thumb as first-order divergence when considering the "effective" wavelength of the second-order sum-frequency term.

The sum- and difference-frequency quadratic terms were computed by WAMIT in the PF solution, but they were not included in ST within HydroDyn. The results show that the quadratic contributions are small at low frequencies (where ST is valid) and increase as frequency increases (Fig. 3). Thus, the quadratic terms have an influence only at the higher frequencies where ST is less valid anyway.

Forces for Specific Sea States

So far, only the normalized force magnitudes have been considered. The actual force on the cylinder can be derived for specific sea states. A range of different sea states were analyzed to understand the differences between the two approaches in calculating the actual forces on the cylinder. Wave frequency and height from sea states, ranging from mild (at 0.5 Hz and 0.09 m) to severe (at 0.059 Hz and 15.24 m), were taken from Jonkman (2010), as shown in Table 2. These sea states were used to dimensionalize the data in Fig. 2 by multiplying the first-order terms by the wave amplitude and by multiplying the second-order terms by the wave amplitude squared (Fig. 4).

Table 2. Wave height for various sea states, from 1 as a mild sea state to 8 as the most severe (Jonkman, 2010)

Sea State	Period (s)	Frequency (Hz)	Wave Height (m)
1	2.0	0.500	0.09
2	4.8	0.208	0.67
3	6.5	0.154	1.40
4	8.1	0.123	2.44
5	9.7	0.103	3.66
6	11.3	0.088	5.49
7	13.6	0.073	9.14
8	17.0	0.059	15.24

The first-order force amplitude data in Fig. 4 shows that the ST and PF solutions do not match at the lowest sea state (1) because of the long wavelength approximation in ST. It is necessary to consider diffraction to properly predict the forces occurring at mild sea states. At less mild, middle, and severe sea states (2–8), ST and PF predict similar first-order force amplitudes.

Second-order sum-frequency effects are significant compared to first-order terms for the most severe sea states (7–8). For the middle sea states (3–6), ST gives a lower second-order sum-frequency force than the PF total because of the importance of diffraction and the quadratic terms in the PF solution at the corresponding frequencies. For the most severe sea states (7–8), the second-order sum-frequency ST and PF solutions approaches are similar because quadratic and diffraction contributions are small.

The second-order difference-frequency force, only calculated by PF, is small for all sea states, but is most significant relative to other forces at mild sea state 2.

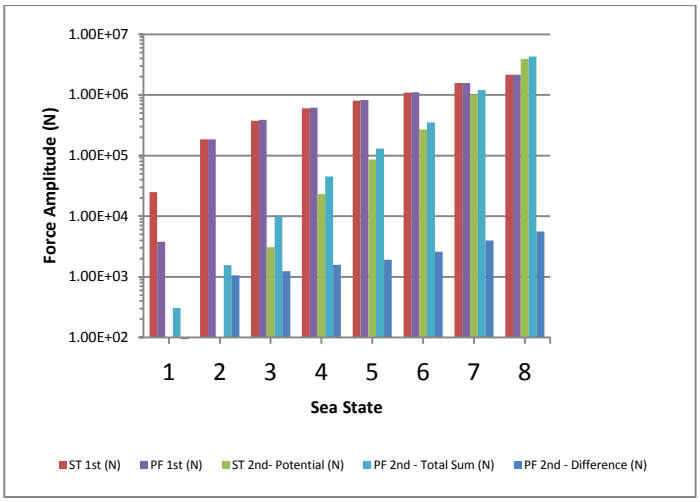

Fig 4. Theoretical first- and second-order force amplitudes (on a log scale) in Newtons on the OC3 monopile for a range of different sea states.

CONCLUSION

Predicting hydrodynamic loads on an offshore structure is an important aspect of design. A comparative study was initiated to better understand the applicability of the two most common methods used to compute hydrodynamic loads in engineering tools.

ST is a simplified model, but it can be applied for thin structures at low wave frequencies. Based on a comparison to PF and confirming known theory, first-order forces can be approximated using ST when the cylinder diameter-to-wavelength ratio is less than 0.2. Second-order sum-frequency forces from ST were consistent with PF solutions following the same rule of thumb based on the "effective" wavelength of the second-order term. At larger ratios, the results from PF and ST diverge for both the first- and second-order solutions.

The separate contributions of the second-order potential and the quadratic interaction of first-order terms to the second-order PF solution were analyzed because the ST solution in HydroDyn does not consider the quadratic terms. The quadratic terms are small at small frequencies or small diameter-to-wavelength ratios, and they increase at higher frequencies and ratios. This increase indicates that ST can approximate PF at low frequencies and low diameter-to-wavelength ratios when (1) the quadratic sum-frequency term is small relative to the total sum-frequency second-order force and (2) the difference-frequency force is negligible. The current ST implementation in HydroDyn can be used to calculate second-order terms at low frequencies where there are severe sea states and the second-order terms are most important, but additional consideration is required for quadratic and diffraction effects in middle sea states.

FUTURE WORK

Now that confidence has been gained in the hydrodynamic models when applied to a simple monopile structure, further studies can involve more complex systems and conditions. This can include modeling different substructure geometries and considering irregular sea states. Future work could also look at whether using a smaller (and frequency-dependent) added-mass coefficient could better match ST to PF at high frequencies.

ACKNOWLEDGEMENTS

This work was supported by the U.S. Department of Energy under Contract No. DE-AC36-08GO28308 with the National Renewable Energy Laboratory. Funding for the work was provided by the DOE Office of Energy Efficiency and Renewable Energy, Wind and Water Power Technologies Office and by the U.S. Department of Energy, Office of Science, Office of Workforce Development for Teachers and Scientists (WDTS) under the Science Undergraduate Laboratory Internship (SULI) program.

APPENDIX

From Morison's equation for a vertical cylinder, the inertial surge force amplitude per unit length along the cylinder is proportional to the amplitude of the undisturbed water particle (fluid) acceleration normal to the cylinder:

$$dF_{Inertia}/dz(z,\omega) = (1 + C_A)\rho_f \pi R^2 a_f(z,\omega) \qquad (1)$$

where z is the local depth, ω is the first-order wave frequency in rad/s, C_A is the coefficient of added mass, ρ_f is the density of the fluid, R is the radius of the cylinder, and a_f is the amplitude of the undisturbed fluid acceleration normal to the cylinder. For regular waves and finite water depth, the amplitudes of the undisturbed fluid acceleration normal to the cylinder for first-order (linear Airy) and second-order (Stokes) theory are:

$$a_f^{(1)}(z,\omega) = \frac{agk\cosh\big(k(z+h)\big)}{\cosh(kh)} \tag{2}$$

$$a_f^{(2-)}(z,\omega) = 0 \tag{3}$$

$$a_f^{(2+)}(z,\omega) = \frac{a^2 3gk^2\cosh\big(2k(z+h)\big)}{2\,(\sinh(kh))^3\cosh(kh)} \tag{4}$$

where a is the first-order wave elevation amplitude (half the wave height), g is the gravitational constant, h is the water depth, and k is the wave number, related to ω by the dispersion relationship, $\omega = \sqrt{gk\tanh(kh)}$. The first-order wavelength is given by $\lambda = \frac{2\pi}{k}$. The second-order difference-frequency (mean-drift) fluid acceleration is zero because the quadratic interaction of first-order quantities was not considered in this theoretical solution. Although the first-order fluid acceleration oscillates at ω, the second-order sum-frequency fluid acceleration oscillates at 2ω.

The theoretical first- and second-order inertial surge force amplitudes were derived by integrating the inertial force term from Morison's equation, Eq. 1, along the length of the cylinder from the seabed ($z = -h$) to the still-water level ($z = 0$). For regular waves and finite water depth, the inertial surge force amplitudes based on the first-order (linear Airy) and second-order (Stokes) undisturbed fluid accelerations normal to the cylinder (Eqs. 2–4) are:

$$F_{Inertia}^{(1)}(\omega) = a(1+C_A)\rho_f\pi R^2 g\tanh(kh) \tag{5}$$

$$F_{Inertia}^{(2-)}(\omega) = 0 \tag{6}$$

$$F_{Inertia}^{(2+)}(\omega) = \frac{a^2 3(1+C_A)\rho_f\pi R^2 gk}{2\,(\sinh(kh))^2} \tag{7}$$

Again, the second-order difference-frequency (mean-drift) force is zero because the quadratic interaction of first-order quantities was not considered in this theoretical solution. Like the fluid acceleration, the first-order force oscillates at ω and the second-order sum-frequency force oscillates at 2ω.

REFERENCES

Faltinsen, OM (1990). *Sea Loads on Ships and Offshore Structures*, Cambridge, United Kingdom: Cambridge University Press.

Jonkman, J, and Musial, M (2010). *Offshore Code Comparison Collaboration (OC3) for IEA Task 23 Offshore Wind Technology and Deployment*, Golden, CO: National Renewable Energy Laboratory.

Jonkman, JM (2010). *Definition of the Floating System for Phase IV of OC3*, Golden, CO: National Renewable Energy Laboratory.

Jonkman, JM, Roberston, AN, and Hayman, GJ (2014). *HydroDyn User's Guide and Theory Manual*, Golden, CO: National Renewable Energy Laboratory.

Lee, C (1995). *WAMIT Theory Manual*, Cambridge, MA: Massachusetts Institute of Technology, Department of Ocean Engineering.

Musial, W, and Ram, B (2010). *Large-Scale Offshore Wind Power in the United States,* Golden, CO: National Renewable Energy Laboratory.